Energy-based modeling and robust position control of a dielectric elastomer cardiac assist device ⋆

Amal Hammoud * Ning Liu ** Yann Le Gorrec *
Yoan Civet * Yves Perriard *****

* *SUPMICROTECH, CNRS, institut FEMTO-ST, F-25000 Besançon, France (e-mails: amal.hammoud@femto-st.fr; yann.le.gorrec@ens2m.fr)*
** *Université de Franche-Comté, SUPMICROTECH, CNRS, institut FEMTO-ST, F-25000 Besançon, France (e-mail: ning.liu@femto-st.fr)*
*** *Integrated Actuators Laboratory, École Polytechnique Fédérale de Lausanne, 1015 Lausanne, Switzerland (e-mails: yoan.civet@epfl.ch; yves.perriard@epfl.ch)*

Abstract: This paper is concerned with the port Hamiltonian modeling and control of a dielectric elastomer actuator used for a cardiac assistance device. The proposed non-linear model is identified under different applied voltages and pressures, and validated against experimental results with relative errors of less than 0.3%. Subsequently, two passivity-based controllers are designed to stabilize the actuator at a desired position. The first controller is designed using control by interconnection. The second one considers additional integral action to reject disturbances while preserving the passivity of the closed-loop system.

Keywords: Dielectric elastomer actuators, port-Hamiltonian systems, passivity-based control, integral action.

1. INTRODUCTION

In the past two decades, there has been a remarkable research interest in soft smart actuators using electro-active polymers (EAP), especially dielectric elastomer actuators (DEAs). A DEA is generally composed of an elastomeric material sandwiched between two compliant electrodes. When an electric voltage is applied to the electrodes, the elastomeric material is polarized and undergoes deformation. The DEAs have particularly been applied in the field of biomedical robotics due to its advantages such as large deformation, rapid response time, high compliance, low power consumption, and good biocompatibility (Gupta et al., 2019). In this paper we consider a particular application of DEAs to cardiac surgery. It has indeed been shown in (Almanza et al., 2021) that one can replace a segment of the aorta with a tubular DEA in order to ease heart failure, as depicted in Fig. 1. In this application the tubular DEA is initially pre-stretched by blood pressure. During the diastolic phase, a high voltage (kilo-volt) is applied to the compliant electrodes, inducing a Maxwell stress that compresses the elastomer along the thickness direction. From the fact that the elastomer material is incompressible, the volume of the actuator is conserved. The DEA thus expands along the radial direction, reducing internal blood pressure. Subsequently, at the end of systole, the DEA is deactivated and contracts, enhancing the recoil force of the aorta.

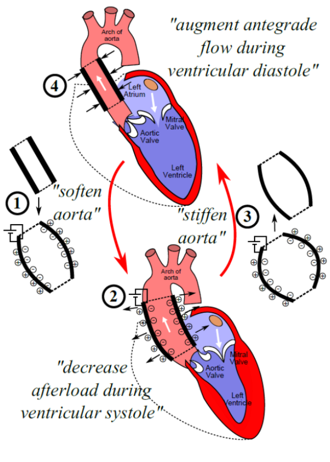

Fig. 1. Schematic representation of a tubular DEA cardiac assist device in augmented aorta (Almanza et al., 2021).

Despite the aforementioned considerable advantages, DEAs exhibit inherent limitations, particularly with respect to electro-mechanical instability, the major of which is referred to as snap-through instability (Zhao et al., 2007; Xu et al., 2010). It comes from the applied interaction between the electric field and the deformation of the

⋆ This work has been supported by the EIPHI Graduate School (contract ANR-17-EURE-0002). The third author acknowledges the MSCA Project MODCONFLEX 101073558 and the ANR Project IMPACTS ANR-21-CE48-0018. The fourth and fifth authors acknowledge the Werner Siemens Foundation.

DEA. With the electric field, the thickness of the DEA decreases due to the aforementioned Maxwell stress. The reduction of the actuator's thickness leads to an increase of the electric field, causing further thinning of the actuator until it collapses. This well-known phenomenon has been observed and analyzed from a material point of view in (Zhu et al., 2010; Suo, 2010; Dorfmann and Ogden, 2019; Liu et al., 2021b). To avoid this instability in the cardiac assist device (illustrated in Fig. 1.), it has been proposed in (Martinez et al., 2021) to place a rigid tube outside the tubular DEA to limit the radial displacement without triggering the snap effect. However, this rigid protection limits the maximum displacement, reduces the achievable energy and compliance, and results in a non-soft system. To tackle this, we propose to stabilize the tubular DEA in closed-loop using a dynamic controller, instead of the rigid protection. The idea is to modify both the stability of this unstable system and its closed-loop performances using appropriate control strategies.

Several models of DEAs have been proposed in the literature, their complexity depending on the assumptions on the considered phenomena such as material viscoelasticity, nonlinear deformations *etc.* They are divided into lumped parameter models and distributed parameter models. The former considers the DEA as a discrete system, where the properties of the elastomeric material and the electromechanical effects are represented by piecewise constant parameters, see (Rizzello et al., 2014; Bernat et al., 2020; Kaaya et al., 2022, 2023). These models are relatively simple and easy to use for simulation and control, but they may neglect some phenomena. On the other hand, distributed parameter models (Garnell, 2020) take into account the spatial distribution of the elastomeric material properties. They describe more precisely the behavior of DEAs by considering infinitesimal variations in forces, deformations, and electromechanical interactions.

From both theoretical and practical concerns, and in order to simplify the simulation and control implementation, we start with a nonlinear and lumped parameter model based on previous work (Liu et al., 2022), that only focuses on the deformation of the center of the tube. From the fact that DEAs are multiphysical, the current model is formulated under the port-Hamiltonian framework, which is an energy-based modeling to deal with interactions in different physical domains (Duindam et al., 2009). This framework has been applied to model EAP actuators such as piezoelectric actuators in (Voß, 2010), ionic polymer-metal composite actuators in (Liu et al., 2021a) and the DEAs in (Rizzello et al., 2017). Furthermore, port-Hamiltonian system (PHS) formulations provide a clear physical interpretation for control design. The Hamiltonian (*i.e.*, total stored energy) is a good Lyapunov function candidate and the system is passive in nature. Therefore, passivity-based control methodologies such as Control by Interconnection (CbI) and Interconnection and Damping Assignment Passivity Based Control (IDA-PBC) (Ortega et al., 2001) have been investigated for both lumped parameter PHS and distributed parameter PHS.

The contributions of this paper with respect to other studies on DEAs under PHS as in (Rizzello et al., 2017) are the following:

(1) We propose a nonlinear port-Hamiltonian model of a clamped-clamped DEA tube and validate the model using experimental data.
(2) A position control based on CbI methodology is designed. Both energy shaping and damping injection are investigated in order to achieve the desired closed loop performances.
(3) An integral action that preserves the PHS structure has been added in closed-loop. This integral part improves the system's robustness to external disturbances.

The paper is organized as follows. Section 2 describes the proposed port-Hamiltonian model of the system. The key parameters of the model are identified in Section 3 and the model is validated from experimental data. Section 4 is concerned with control design. The paper ends with some conclusions and perspectives in Section 5.

2. ENERGY-BASED MODELING

DEAs are multiphysical systems integrating both mechanical and electrical components that are coupled through the generated Maxwell stress. When it comes to our problem, the DEA tube is firstly pre-stretched by the inner pressure $F_p(t)$, and then actuated with the applied voltage $U(t)$. The assumptions made for the energy-based modeling are the following:

- The material of DEA is isotropic and incompressible.
- The elastomer is considered ideal, which means that the electric permittivity (i.e. the product of the vacuum permittivity ϵ_0 and the relative dielectric permittivity ϵ_r) is constant.
- The deformation is homogeneous and is supposed to be radial axisymmetric.
- The mass of the DEA is concentrated in the studied part.

From the last two assumptions, we can represent our model as nonlinear mass spring damper system as in Fig. 2, where m represents the mass of the DEA. The two symmetric springs of stiffness K_1 stem from the actuator longitudinal deformation, l_0 and $L(t)$ being the initial and actual lengths. The vertical spring of stiffness K_2 stands for the radial deformation. r_0 and $R(t)$ refer to the initial and actual radius of the DEA tube, respectively. $F_e(t)$ represents the electrostatic force that depends on both the deformation and the applied voltage.

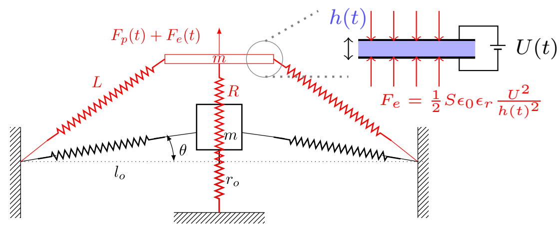

Fig. 2. Simplified lumped parameter model of a radial axisymmetric DEA tube.

Given $l(t) = L(t) - l_0$ and $r(t) = R(t) - r_0$, the geometric relation between $r(t)$ and $l(t)$ writes:

$$r(t) = \sqrt{(l_0 + l(t))^2 - l_0^2}. \tag{1}$$

Define $p(t) = m\dot{r}(t)$ the momentum of the tube, one obtains:

$$\dot{l} = \dot{L} = \frac{\partial L}{\partial r}\dot{r} = \frac{r}{L}\frac{p}{m}. \tag{2}$$

According to Fig. 2, the equation of motion for the mass gives:

$$\begin{aligned}\dot{p} &= -2K_1 l \sin\theta - K_2 r - R_{es}\dot{r} + F_e(t) + F_p(t)\\ &= -2K_1 l \sin\theta - K_2 r - R_{es}\dot{r} + \frac{1}{2}S\epsilon_0\epsilon_r\frac{U^2}{h(t)^2} + F_p(t)\\ &= -2\frac{r}{L}K_1 l - K_2 r - R_{es}\frac{p}{m} + \alpha L^3 R^3 U(t)^2 + F_p(t), \quad (3)\end{aligned}$$

where R_{es} is the dissipation that represents the linear viscoelasticity of the DEA tube, $\alpha = \frac{1}{2}\frac{\epsilon_0\epsilon_r}{V^2}$ is a constant, with V denoting the volume of the tube.

The Hamiltonian of the system is :

$$H(t) = \frac{1}{2}\frac{p(t)^2}{m} + K_1 l(t)^2 + \frac{1}{2}K_2 r\,(l(t))^2. \tag{4}$$

Choosing the energy variables as $x_1 = l$ and $x_2 = p$, equation (2) and (3) can be reformulated under the PHS in the following explicit input-state-output form:

$$\begin{cases}\dot{x}(t) = (J(x) - R_h)\nabla_x H(x) + g_1(x)u_1(t) + g_2 u_2(t),\\ y_1(t) = g_1^T(x)\nabla_x H(x),\\ y_2(t) = g_2^T(x)\nabla_x H(x),\end{cases} \tag{5}$$

where $J(x) = \begin{bmatrix} 0 & \frac{r}{L}(x_1)\\ -\frac{r}{L}(x_1) & 0\end{bmatrix}$ is the skew symmetric interconnection matrix and $R_h = \begin{bmatrix}0 & 0\\ 0 & R_{es}\end{bmatrix}$ is symmetric and non negative dissipation matrix. The co-energy variables are derived from the partial derivative of the Hamiltonian, which gives:

$$\nabla_x H(x) = \begin{bmatrix} 2K_1 x_1 + K_2 L(x_1)\\ \frac{1}{m}x_2\end{bmatrix}. \tag{6}$$

We consider $u_1(t) = U(t)^2$ and $u_2(t) = F_p(t)$ as two inputs with input matrices $g_1(x) = \begin{bmatrix}0\\ \alpha L(x_1)^3 R(x_1)^3\end{bmatrix}$ and $g_2 = \begin{bmatrix}0\\1\end{bmatrix}$. Hence, y_1 and y_2 are the power-conjugated outputs.

3. PARAMETERS IDENTIFICATION

Several physical parameters in the nonlinear PHS model (5) are unknown and necessitate to be identified according to experimental measurements. The experimental setup has been developed at the Integrated Actuators Laboratory of EPFL and is depicted in Fig. 3. It consists of a DEA tube, a piston that exerts pressure input, two wires that apply voltage to the DEA, a pressure sensor hidden below, and a 2D laser sensor to measure the radial profile deformation.

Similar to the strategy presented in (Liu et al., 2022), the identification process is conducted in two steps. Firstly, the DEA tube is actuated only by applying a pressure as illustrated in Fig. 4a. According to the deformation at the middle point of the tube (blue line in Fig. 4b), the DEA is in a quasi-static state. One can then identify the stiffness K_1 and K_2 of the two springs. This is realized using the Parameter Estimator application in @Simulink. The optimization method is the Nonlinear least squares and the applied algorithm is Trust-Region-Reflective. The relative errors between the simulation results and measurements of the deformation at middle point are presented in Fig. 5, and are less than 0.3%.

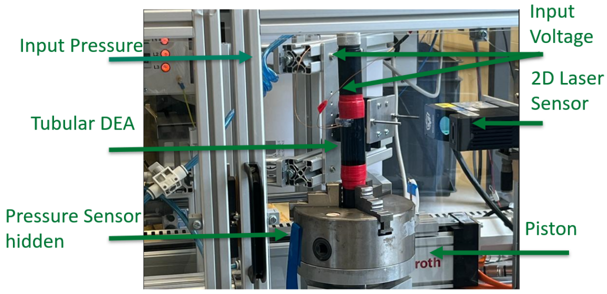

Fig. 3. Experimental setup of the tubular DEA under measurement.

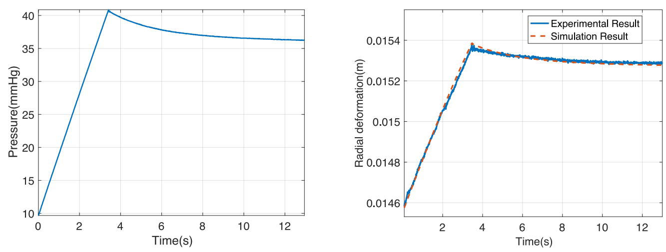

(a) Input pressure. (b) Middle point deformation.

Fig. 4. Identification of K_1 and K_2 with applied pressure.

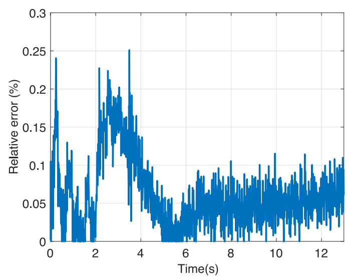

Fig. 5. Relative errors for the identification of K_1 and K_2.

In a second instance, with the piston staying at previous fixed position, we apply a step voltage of 5 kV in order to identify the dissipation parameter R_{es} and the parameter α of the input matrix. The input signals are shown in Fig. 6. The comparison between the experiment and simulation results are depicted in Fig. 7a. The corresponding relative errors are presented in Fig. 7b, which are less than 0.3%.

The resulting values of the identified parameters are listed in Table 1. The validation of the model is then carried out with a step voltage of 4 kV. According to the relative errors illustrated in Fig. 8, the proposed model can approximate the behavior of DEA tube within a certain deformation range.

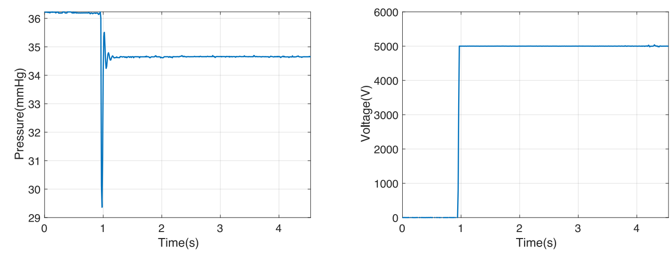

(a) Input pressure. (b) Input Voltage.

Fig. 6. Input signals for the identification of R_{es} and α.

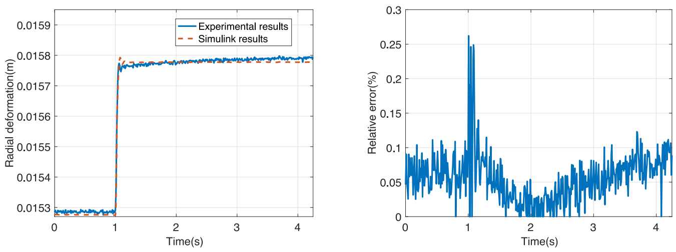

(a) Middle point deformation. (b) Relative errors.

Fig. 7. Comparison between measurements and simulation results for identification of R_{es} and α.

Table 1. Identified parameters of DEA tube.

Parameters	Values	Units
K_1	21003	kN/m
K_2	84.072	kN/m
α	5.514	kF/m^7
R_{es}	754	$N \cdot s/m$

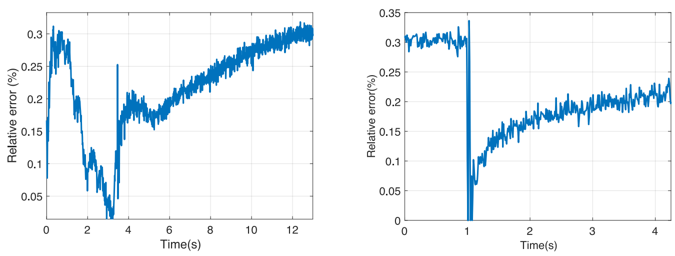

(a) On the validation of K_1 and K_2. (b) On the validation of R_{es} and α.

Fig. 8. Relative errors on the validation with step voltage of 4kV.

4. PASSIVITY-BASED CONTROL

The objectives of the controller are twofold. On one hand, we would like to assign the desired position of the DEA tube with a dynamic controller and ensure the closed-loop stability. Moreover, due to the fact that model uncertainties and external disturbances are inescapable in practical applications for DEAs, another objective is to improve the robustness of the closed-loop system to these perturbations. In what follows, we study two controllers, CbI and CbI with integral action, which helps to achieve these two objectives and preserve the PHS structure of the system.

4.1 Control by interconnection

The control by interconnection consists in connecting a passive controller to the plant in a power-preserving way, as illustrated in Fig. 9. The controller is designed to be a PHS. Therefore the closed-loop system is again a PHS (van der Schaft, 2017).

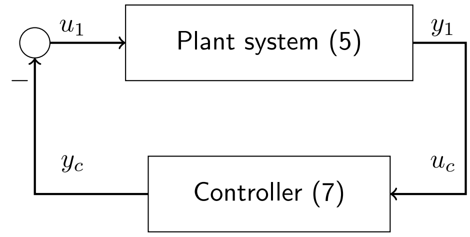

Fig. 9. Control by interconnection illustration.

We propose the following structure for the controller:

$$\begin{cases} \dot{x}_c = (J_c(x_c) - R_c(x_c))\, \nabla_{x_c} H_{c1}(x_c) + g_c(x_c) u_c, \\ y_c = g_c^T(x_c) \nabla_{x_c} H_{c1}(x_c), \end{cases} \tag{7}$$

where x_c denotes the control state, H_{c_1} is the controller Hamiltonian, $J_c(x_c) = -J_c(x_c)^T$, $R_c(x_c) = R_c(x_c)^T \geq 0$, $g_c(x_c)$ represents the input matrix of the controller, and u_c and y_c are its power-conjugated input and output. It is associated to a Hamiltonian $H_{c1}(x_c(t))$.

The passive interconnection between the plant (equation (5)) and the controller (equation (7)) writes:

$$u_1 = -y_c, \tag{8}$$

$$y_1 = u_c, \tag{9}$$

such that:

$$u_1^T(t) y_1(t) + u_c^T(t) y_c t = -y_c^T y_1 + y_1^T y_c = 0. \tag{10}$$

Therefore, the closed-loop system reads:

$$\begin{bmatrix} \dot{x} \\ \dot{x}_c \end{bmatrix} = \begin{bmatrix} J(x) - R_h & -g_1(x) g_c^T(x_c) \\ g_c(x_c) g_1^T(x) & J_c(x_c) - R_c(x_c) \end{bmatrix} \begin{bmatrix} \nabla_x H_d(x, x_c) \\ \nabla_{x_c} H_d(x, x_c) \end{bmatrix}, \tag{11}$$

$$\begin{bmatrix} y_1 \\ y_c \end{bmatrix} = \begin{bmatrix} g_1(x)^T & 0 \\ 0 & g_c^T(x_c) \end{bmatrix} \begin{bmatrix} \nabla_x H_d(x, x_c) \\ \nabla_{x_c} H_d(x, x_c) \end{bmatrix}, \tag{12}$$

with closed-loop Hamiltonian as:

$$H_d(x, x_c) = H(x(t)) + H_{c_1}(x_c(t)). \tag{13}$$

We would like to get an energy function in terms of the plant state x only, *i.e.* $H_d(x)$, so that we can assign the minimum of H_d at the desired position and characterize it in terms of the plant state. To achieve this, we look for structural invariants, also called Casimir functions C as proposed in (Ortega et al., 2001). It is an invariant on a submanifold of the (x, x_c) space parameterized by x. It is looked for in a linear format as:

$$x_c = F(x) - C. \tag{14}$$

From the condition that $\frac{dC}{dt} = 0$, we obtain:

$$\begin{bmatrix} \frac{\partial F}{\partial x}^T(x), & -I \end{bmatrix} \begin{bmatrix} J(x) - R_h & -g_1(x) g_c^T(x_c) \\ g_c(x_c) g_1^T(x) & J_c(x_c) - R_c(x_c) \end{bmatrix} = 0, \tag{15}$$

which yields the following matching equations:

$$\frac{\partial F}{\partial x}^T(x)J(x)\frac{\partial F}{\partial x}(x) = J_c(x_c), \tag{16}$$

$$R_h\frac{\partial F}{\partial x}(x) = 0, \tag{17}$$

$$R_c(x_c) = 0, \tag{18}$$

$$\frac{\partial F}{\partial x}^T(x)J(x) = g_c(x_c)g_1^T(x). \tag{19}$$

The solution of matching equations (16)-(19) leads to $J_c = 0$, $R_c = 0$, and

$$F(x_1) = \beta x_1, \tag{20}$$

with

$$\beta = \frac{L}{r}\alpha L^3 R^3 g_c. \tag{21}$$

Therefore, if we properly initialize x_c such that $C = 0$, we get always an algebraic relation between x_c and x_1 that writes:

$$x_c = \beta x_1. \tag{22}$$

We choose :

$$H_{c_1} = (K_\alpha - K_1)\,l^2 - 2K_\alpha l l^* + K_\alpha (l^*)^2 - K_2 r r^* + \frac{1}{2}K_2\,(r^*)^2\,, \tag{23}$$

such that :

$$H_d = K_\alpha (l-l^*)^2 + \frac{p^2}{2m} + \frac{1}{2}K_2(r-r^*)^2, \tag{24}$$

with K_α the desired stiffness of the longitudinal springs in closed-loop.

The input is hereby:

$$\begin{aligned} u = \Big(&-2\,(K_\alpha - K_1)\,x_1 + 2K_\alpha l^* + K_2 r^* \frac{L}{r}(x_1) \\ &-R_d\frac{x_2}{m}\Big)\,\frac{1}{\frac{L}{r}\alpha L^3 R^3}. \end{aligned} \tag{25}$$

The first term of u works as energy shaping that modifies both the closed-loop stiffness and equilibrium point, and the second term is a damping injection with R_d a closed-loop dissipation parameter that is free to choose.

The equivalent closed-loop system writes:

$$\dot{x} = (J(x) - R_n)\,\nabla_x H_d(x), \tag{26}$$

with $R_n = \begin{bmatrix} 0 & 0 \\ 0 & (R_d + R_{es}) \end{bmatrix}$ and

$$\nabla_x H_d(x) = \begin{bmatrix} 2K_\alpha(x_1 - x_1^*) + K_2 L\left(1 - \dfrac{r^*}{r}\right) \\ \dfrac{1}{m}x_2 \end{bmatrix}.$$

Given a desired radial deformation of 0.1 mm, by assigning $K_\alpha = 5 \times 10^7$ and $R_d = 10^4$, the simulation results are presented in Fig. 10a. The control input is illustrated in Fig. 10b. One can see that the control input corresponds to a steady input voltage of $U = 2.4$kV, which is within an admissible range.

4.2 Control by interconnection adding an integrator

The controller designed by CbI methodology focuses on stabilizing the closed-loop system (26) to a given set point for x_1. However, it cannot reject the error that occurs in the presence of disturbances, indicating that the previous closed-loop Hamiltonian H_d cannot be considered as a

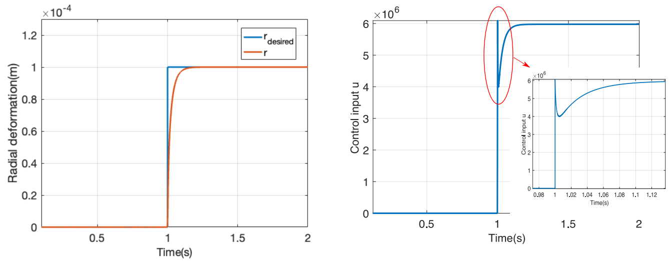

(a) Radial deformation (b) Input signal.

Fig. 10. Simulation results for CbI.

Lyapunov candidate for the perturbed system. This is due to the fact that our input-output pair is no longer passive. Therefore, it is necessary to add a robust controller in the closed-loop.

We consider a constant disturbance force d_a adding on the same port of the input, which is formulated as:

$$\begin{bmatrix} \dot{x}_1 \\ \dot{x}_2 \end{bmatrix} = (J(x) - R_n)\begin{bmatrix} \nabla_{x_1} H_d(x) \\ \nabla_{x_2} H_d(x) \end{bmatrix} + \begin{bmatrix} 0 \\ u_i - d_a \end{bmatrix}, \tag{27}$$

where u_i is the robust control input. It has been proposed in (Ferguson et al., 2017) and (Ferguson, 2018) that adding an integral action to (27) can both reject the disturbance and preserve the passivity of the closed-loop system. The restrictions of applying integral action can be avoided by relaxing the structure of the storage function associate with the integral action scheme. In particular the storage function can mix the plant state x_2 with the integrator states x_{ci} as:

$$H_c\,(x_2, x_{ci}) = \frac{1}{2} \parallel \gamma x_2 - x_{ci} \parallel^2 K_i, \tag{28}$$

with γ and K_i the tuning parameters of the controller.

The closed-loop system containing both the CbI and the integral action reads:

$$\begin{bmatrix} \dot{x}_1 \\ \dot{x}_2 \\ \dot{x}_{ci} \end{bmatrix} = \begin{bmatrix} \multicolumn{2}{c}{J(x) - R_n} & \begin{matrix} \gamma\frac{r}{L} \\ -\gamma R_d + \eta \end{matrix} \\ -\gamma\frac{r}{L} & -\gamma R_d - \eta & -\gamma^2 R_d - \gamma\eta \end{bmatrix}\begin{bmatrix} \nabla_{x_1} H_{cl} \\ \nabla_{x_2} H_{cl} \\ \nabla_{x_{ci}} H_{cl} \end{bmatrix} + \begin{bmatrix} d_a \\ 0 \\ 0 \end{bmatrix} \tag{29}$$

with

$$H_{cl}(x, x_{ci}) = H_d\,(x) + H_c\,(x_2, x_{ci})\,. \tag{30}$$

The partial derivatives of the Hamiltonian $H_{cl}(x, x_{ci})$ are calculated as:

$$\nabla_{x_1} H_{cl} = \nabla_{x_1} H_d, \tag{31}$$

$$\nabla_{x_2} H_{cl} = \nabla_{x_2} H_d + \gamma K_i\,(\gamma x_2 - x_{ci})\,, \tag{32}$$

$$\nabla_{x_{ci}} H_{cl} = -K_i\,(\gamma x_2 - x_{ci})\,. \tag{33}$$

The integral dynamics is formulated as:

$$\begin{aligned} \dot{x}_{ci} =& -\gamma\frac{r}{L}\nabla_{x_1} H_{cl} - (\gamma R_d + \eta)\,\nabla_{x_2} H_{cl} \\ &- \left(\gamma^2 R_d + \gamma\eta\right)\nabla_{x_{ci}} H_{cl} \\ =& -\gamma\frac{r}{L}\nabla_{x_1} H_d - (\gamma R_d + \eta)\,\nabla_{x_2} H_d, \end{aligned} \tag{34}$$

with $\nabla_{x_1} H_d$ and $\nabla_{x_2} H_d$ detailed in equation (26). From the dynamics of x_2 in equation (29), the integral action law is:

$$u_i = -\eta K_i\,(\gamma x_2 - x_{ci})\,. \tag{35}$$

We keep with the previous control scenario as in subsection 4.1. From $t = 2.5$s a perturbation is added, which is presented in Fig. 11a. With controller parameters $R_d = 10^6$, $\gamma = 1$, $\eta = 1$ and $K_i = 10$, one can see that the proposed control u_i can reject the disturbance.

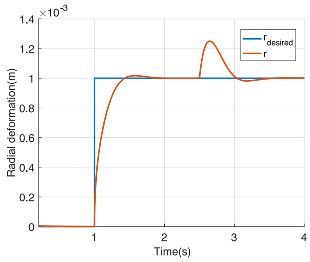

(a) Radial deformation.

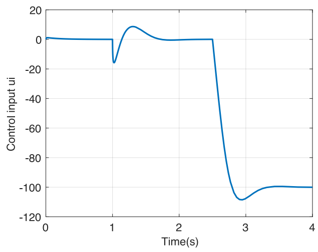

(b) Control input u_i.

Fig. 11. Simulation results for CbI and integrator.

5. CONCLUSION AND PERSPECTIVES

In this paper, we have proposed a nonlinear dynamic model of a DEA tube. This model is characterized by two linear springs along the longitudinal direction, and a vertical one, actuated by an electrostatic force that depends on the actuator's thickness. This electromechanical coupling is a source of instability. The parameters are presented in a lumped parameter form, and the system is represented in the port-Hamiltonian framework. Unknown physical parameters have been identified with a step voltage of 5 KV, and have been validated with another step voltage of 4 KV. Subsequently, passivity-based controllers, *i.e.* control by interconnection with and without integral action, have been applied on the proposed model. The dynamic controller aims to achieve the desired position in a reasonable response time, and to reject external disturbance forces.

Future works are to implement the designed controller on the experimental setup, and enhance the model by considering the electric dynamics, nonlinear material properties and then extend both the model and control to distributed parameter systems.

REFERENCES

Almanza, M., Clavica, F., Chavanne, J., Moser, D., Obrist, D., Carrel, T., Civet, Y., and Perriard, Y. (2021). Feasibility of a dielectric elastomer augmented aorta. *Advanced science*, 8(6), 2001974.

Bernat, J., Kolota, J., and Rosset, S. (2020). Identification of a nonlinear dielectric elastomer actuator based on the harmonic balance method. *IEEE/ASME Transactions on Mechatronics*, 26(5), 2664–2675.

Dorfmann, L. and Ogden, R.W. (2019). Instabilities of soft dielectrics. *Philosophical Transactions of the Royal Society A*, 377(2144), 20180077.

Duindam, V., Macchelli, A., Stramigioli, S., and Bruyninckx, H. (2009). *Modeling and control of complex physical systems: the port-Hamiltonian approach*. Springer Science & Business Media.

Ferguson, J. (2018). *Robust Control of Port-Hamiltonian Systems*. Ph.D. thesis, The University of Newcastle.

Ferguson, J., Donaire, A., and Middleton, R.H. (2017). Integral control of port-hamiltonian systems: Nonpassive outputs without coordinate transformation. *IEEE Transactions on Automatic Control*, 62(11), 5947–5953.

Garnell, E. (2020). *Dielectric elastomer loudspeakers: models, experiments and optimization*. Ph.D. thesis, Institut polytechnique de Paris.

Gupta, U., Qin, L., Wang, Y., Godaba, H., and Zhu, J. (2019). Soft robots based on dielectric elastomer actuators: A review. *Smart Materials and Structures*, 28(10), 103002.

Kaaya, T., Venkatraman, R.J., and Chen, Z. (2023). Physics-based modeling of dielectric elastomer enabled cuff device. In *2023 American Control Conference (ACC)*, 131–136. IEEE.

Kaaya, T., Wang, S., Cescon, M., and Chen, Z. (2022). Physics-lumped parameter based control oriented model of dielectric tubular actuator. *International Journal of Intelligent Robotics and Applications*, 6, 397–413.

Liu, N., Martinez, T., Walter, A., Civet, Y., and Perriard, Y. (2022). Control-oriented modeling and analysis of tubular dielectric elastomer actuators dedicated to cardiac assist devices. *IEEE Robotics and Automation Letters*, 7(2), 4361–4367.

Liu, N., Wu, Y., and Le Gorrec, Y. (2021a). Energy-based modeling of ionic polymer–metal composite actuators dedicated to the control of flexible structures. *IEEE/ASME Transactions on Mechatronics*, 26(6), 3139–3150.

Liu, Z., McBride, A., Sharma, B.L., Steinmann, P., and Saxena, P. (2021b). Coupled electro-elastic deformation and instabilities of a toroidal membrane. *Journal of the Mechanics and Physics of Solids*, 151, 104221.

Martinez, T., Chavanne, J., Walter, A., Civet, Y., and Perriard, Y. (2021). Design and modelling of a tubular dielectric elastomer actuator with constrained radial displacement as a cardiac assist device. *Smart Materials and Structures*, 30, 105024.

Ortega, R., Van Der Schaft, A.J., Mareels, I., and Maschke, B. (2001). Putting energy back in control. *IEEE Control Systems Magazine*, 21(2), 18–33.

Rizzello, G., Naso, D., and Seelecke, S. (2017). A thermodynamically consistent port-hamiltonian model for dielectric elastomer membrane actuators and generators. *IFAC-PapersOnLine*, 50, 4855–4862.

Rizzello, G., Naso, D., York, A., and Seelecke, S. (2014). Modeling, identification, and control of a dielectric electro-active polymer positioning system. *IEEE Transactions on Control Systems Technology*, 23(2), 632–643.

Suo, Z. (2010). Theory of dielectric elastomers. *Acta Mechanica Solida Sinica*, 23(6), 549–578.

van der Schaft, A. (2017). *L2-Gain and Passivity Techniques in Nonlinear Control*. Springer International Publishing, 3 edition.

Voß, T. (2010). Port-hamiltonian modeling and control of piezoelectric beams and plates: application to inflatable space structures.

Xu, B.X., Mueller, R., Klassen, M., and Gross, D. (2010). On electromechanical stability analysis of dielectric elastomer actuators. *Applied Physics Letters*, 97.

Zhao, X., Hong, W., and Suo, Z. (2007). Electromechanical hysteresis and coexistent states in dielectric elastomers. *Physical Review B*, 76, 134113.

Zhu, J., Stoyanov, H., Kofod, G., and Suo, Z. (2010). Large deformation and electromechanical instability of a dielectric elastomer tube actuator. *Journal of Applied Physics*, 108(7).